In vivo quantification of hypoxic and metabolic status of NSCLC tumors using [18f]hx4 and [18f]fdg-pet/ct imaging

Published OnlineFirst October 14, 2014; DOI: 10.1158/1078-0432.CCR-14-1524

Clinical Cancer Research

Personalized Medicine and Imaging

In Vivo Quantification of Hypoxic and Metabolic Status of NSCLC Tumors Using [^{18}F]HX4 and [^{18}F]FDG-PET/CT Imaging

Catharina M.L. Zegers[1], Wouter van Elmpt[1], Bart Reymen[1], Aniek J.G. Even[1], Esther G.C. Troost[1], Michel C. Öllers[1], Frank J.P. Hoebers[1], Ruud M.A. Houben[1], Jonas Eriksson[2], Albert D. Windhorst[2], Felix M. Mottaghy[3,4], Dirk De Ruysscher[1,5], and Philippe Lambin[1]

Abstract

Purpose: Increased tumor metabolism and hypoxia are related to poor prognosis in solid tumors, including non–small cell lung cancer (NSCLC). PET imaging is a noninvasive technique that is frequently used to visualize and quantify tumor metabolism and hypoxia. The aim of this study was to perform an extensive comparison of tumor metabolism using 2[^{18}F]fluoro-2-deoxy-D-glucose (FDG)-PET and hypoxia using HX4-PET imaging.

Experimental Design: FDG- and HX4-PET/CT images of 25 patients with NSCLC were coregistered. At a global tumor level, HX4 and FDG parameters were extracted from the gross tumor volume (GTV). The HX4 high-fraction (HX4-HF) and HX4 high-volume (HX4-HV) were defined using a tumor-to-blood ratio > 1.4. For FDG high-fraction (FDG-HF) and FDG high-volume (FDG-HV), a standardized uptake value (SUV) > 50% of SUV_{max} was used. We evaluated the spatial correlation between HX4 and FDG uptake within the tumor, to quantify the (mis)match between volumes with a high FDG and high HX4 uptake.

Results: At a tumor level, significant correlations were observed between FDG and HX4 parameters. For the primary GTV, the HX4-HF was three times smaller compared with the FDG-HF. In 53% of the primary lesions, less than 1 cm^3 of the HX4-HV was outside the FDG–HV; for 37%, this volume was 1.9 to 12 cm^3. Remarkably, a distinct uptake pattern was observed in 11%, with large hypoxic volumes localized outside the FDG-HV.

Conclusion: Hypoxic tumor volumes are smaller than metabolic active volumes. Approximately half of the lesions showed a good spatial correlation between the PET tracers. In the other cases, a (partial) mismatch was observed. The addition of HX4-PET imaging has the potential to individualize patient treatment. *Clin Cancer Res; 20(24); 6389–97. ©2014 AACR.*

Introduction

Lung cancer has the highest death rate among leading cancer types (1). Standard treatment for advanced-stage non–small cell lung cancer (NSCLC) is the combination of radiotherapy and chemotherapy, administered either sequentially or concurrently (2). Tumor cell hypoxia has a negative impact on cancer treatment effectiveness, it promotes resistance to radiotherapy and chemotherapy, increases the metastatic potential, and is therefore related to a poor prognosis (3–5). Tumor hypoxia is present in the majority of NSCLCs, which can be visualized and quantified using functional PET imaging with radiolabeled 2-nitroimidazoles (6, 7).

3-[^{18}F]Fluoro-2-(4-((2-nitro-1*H*-imidazol-1-yl)methyl)-1*H*-1,2,3-triazol-1-yl)propan-1-ol ([^{18}F]HX4) is a relatively new nitroimidazole with attractive pharmacokinetic properties that has successfully completed preclinical and clinical testing (8–10).

In standard clinical practice, a combination of anatomic computed tomography (CT) and functional 2[^{18}F]fluoro-2-deoxy-D-glucose (FDG)-PET imaging is frequently used to visualize, detect, and stage malignancies. In addition, FDG-PET can be used to identify subvolumes with a high metabolism, which are more susceptible to local recurrence after (chemo)radiotherapy (11, 12). Aerts and colleagues

[1]Department of Radiation Oncology (MAASTRO), GROW—School for Oncology and Developmental Biology, Maastricht University Medical Centre, Maastricht, the Netherlands. [2]Department of Radiology & Nuclear Medicine, VU University Medical Centre, Amsterdam, the Netherlands. [3]Department of Nuclear Medicine, Maastricht University Medical Centre, Maastricht, the Netherlands. [4]Department of Nuclear Medicine, University Hospital Aachen, Aachen, Germany. [5]University Hospitals Leuven/KU Leuven, Leuven, Belgium.

Note: Supplementary data for this article are available at Clinical Cancer Research Online (http://clincancerres.aacrjournals.org/).

Corresponding Author: Catharina M.L. Zegers, Maastro Clinic, Dr. Tanslaan 12, 6229ET Maastricht, the Netherlands. Phone: 31-884455666; Fax: 31-884455667; E-mail: karen.zegers@maastro.nl

doi: 10.1158/1078-0432.CCR-14-1524

Published OnlineFirst October 14, 2014; DOI: 10.1158/1078-0432.CCR-14-1524

Translational Relevance

The ultimate goal of cancer treatment is to provide patient-specific treatment based on tumor characteristics. High tumor metabolism and hypoxia are known to cause treatment resistance. Noninvasive imaging of tumor metabolism [2[^{18}F]fluoro-2-deoxy-D-glucose (FDG)-PET] is already frequently performed in standard clinical practice, but imaging of tumor hypoxia (HX4-PET) is still in the clinical research stage. Both modalities provide the opportunity to show tumor characteristics in 3D, which can be used for response prediction and treatment adaptation. Radiotherapy dose painting based on FDG-PET imaging, for example, is already performed in clinical trials. HX4-PET imaging might provide complementary information to FDG-PET; we therefore performed an extensive comparison of the two imaging modalities. This study shows a (partial) spatial mismatch between FDG- and HX4-PET imaging in some non–small cell lung cancers (NSCLC). The addition of HX4-PET imaging in treatment adaptation might therefore have the potential to individualize patient treatment and improve loco-regional control.

(11, 13) showed that the residual tumor volume after radiotherapy is mainly located within the pre-radiotherapy high FDG-uptake volume. However, 30% of the residual volume did not correspond to the high FDG volume. This may be caused by tumor regrowth in pre-radiotherapy hypoxic tumor subvolumes located outside the high FDG volume. Therefore, it is of great interest to investigate the correlation between both unfavorable biologic features (high tumor metabolism, hypoxia) because they can be used to predict treatment outcome. In addition, imaging-derived tumor features have the potential to guide treatment with hypoxic modifiers or radiotherapy dose painting (14–16). The uptake of FDG in the cell is dependent on the overexpression of glucose transporters (GLUT), which can be upregulated in the absence of oxygen, through the HIF1α-mediated pathway (17). This may suggest a possible overlap between volumes of high FDG uptake and tumor hypoxia, even though they represent different biologic properties of tumors.

The aim of this study was to perform an extensive comparison of tumor metabolism, using FDG, and hypoxia, using HX4, to fully characterize the relationship between both PET tracers on a global tumor and voxel level for primary NSCLC and the regional lymph node metastases.

Materials and Methods

Patients

FDG- and HX4-PET/CT images of 25 patients with NSCLC (17 male and 8 female) were acquired before the start of external beam radiotherapy. The average age of the patients was 63 years (range, 40–82 years). Tumor stage ranged from IIB-IV, pathology being adenocarcinoma ($N = 13$), squamous cell carcinoma (SCC; $N = 5$), and large cell carcinoma ($N = 7$). Patients were treated with radical radiotherapy ($N = 3$) or chemoradiation ($N = 22$), with the majority of patients receiving at least one cycle of chemotherapy before PET imaging and before the start of radiotherapy (Supplementary Table S1). PET data were acquired in the translational research part of two phase II trials [PET-Boost, NCT01024829 (18); Nitroglycerin (NCT01210378)], both having identical PET imaging procedures. The clinical trials were approved by the appropriate medical ethical review committee, and all patients provided written informed consent before study entry.

PET/CT imaging

HX4 was produced as described in previous publications (8–10, 19). After intravenous administration of 429 ± 57 MBq HX4, PET/CT imaging was performed at 4 hours postinjection (p.i.) for 20 to 30 minutes in a single bed position centered around the primary tumor. HX4-PET/CT images were acquired on a Gemini TF 64 scanner (Philips Healthcare), with a spatial resolution of approximately 5-mm FWHM. We performed CT-based attenuation correction and scatter correction (SS-SIMUL), and reconstructed PET images using -ordered subset iterative time-of-flight reconstruction technique (BLOB-OS-TF) with three iterations and 33 subsets in a 144 × 144 matrix and voxel sizes of 4 × 4 mm.

The injected activity of FDG was based on the patient's body weight according to the national guidelines (20). PET/CT imaging was performed 1 hour after intravenous administration of FDG. FDG-PET/CT scans were acquired using a Biograph 40 PET/CT scanner (Siemens Healthcare). Scatter and attenuation corrections were applied. PET images were reconstructed using OSEM 2D (Ordered Subset Expectation Maximization, four iterations, eight subsets) and a Gaussian filter of 5 mm. A respiratory correlated CT was performed, with the mid-ventilation scan selected for the attenuation correction and fusion with the FDG-PET.

HX4- and FDG-PET/CT scans were acquired in the same week for all except 1 patient. The median interval between both PET scans was 3 days (range, 1–14 days). No interventions (e.g., radiotherapy or chemotherapy) were performed between the FDG- and HX4-PET scans. Both scans were acquired with the patient positioned in radiotherapy position, on a flat tabletop using a laser alignment system with arms in an arm-support positioned above the head.

Analysis

For all patients, gross tumor volumes (GTV), including the primary lesion (GTV_{prim}) and involved lymph nodes (GTV_{ln}), were defined on the FDG-PET/CT scan by two experienced radiation oncologists in consensus. GTV_{prim} and GTV_{ln} were analyzed separately. Lesions with a size <5 cm^3 were excluded because of potential partial volume effects.

The FDG-PET/CT was rigidly registered to the HX4-PET/CT using registration software developed in-house. The

Published OnlineFirst October 14, 2014; DOI: 10.1158/1078-0432.CCR-14-1524

rigid transformation was determined by the registration of the FDG-CT to the HX4-CT; the same transformation was subsequently applied to the FDG-PET scan and the GTVs. A volume of interest in the aorta was defined as background region.

The maximum and mean standardized uptake values (SUV_{max} and SUV_{mean}), corrected for body weight, were determined within the GTV for both FDG- and HX4-PET. For the HX4-PET, calculations were made of the maximum tumor-to-blood ratio (TBR_{max}), defined as the SUV_{max} in the tumor divided by the SUV_{mean} in the aorta, the HX4 high-fraction (HX4-HF) and HX4 high-volume (HX4-HV), both defined as the fraction/volume of the GTV with a TBR > 1.4. For the FDG-PET, calculations were made of the FDG high-fraction (FDG-HF) and FDG high-volume (FDG-HV) based on the PET-Boost trial strategy, using the GTV volume with an SUV above 50% of the SUV_{max} (18).

This classification for defining HX4-HV and FDG-HV, as a fraction of the total GTV, was used to subdivide regions of a tumor into four classes: (i) FDG-low and HX4-low, (ii) FDG-high and HX4-low, (iii) FDG-low and HX4-high, and (iv) FDG-high and HX4-high. To evaluate the effect of the threshold definition on tumor subdivision, a calculation was made of the average distribution using alternative thresholds. The HX4 threshold varied from TBR > 1.3 to TBR > 1.5; the FDG threshold ranged from SUV > 30% to SUV > 70% of SUV_{max}.

A visual and voxel-wise comparison of the FDG and HX4 uptake within the GTV was performed to compare spatial uptake patterns in the primary lesions. On the basis of the voxel-wise analysis, we separated lesions into three groups. First, in lesions showing a high correlation between the FDG and HX4 uptake, the hypoxic volume was entirely within the high metabolic volume. Second, in lesions showing a moderate correlation between the FDG and HX4 uptake, there was only a partial overlap between the HX4-HV and the FDG-HV. Third, in lesions showing a different uptake pattern between the two tracers, there were two distinct regions of FDG-HV and HX4-HV.

Statistical analysis

Mean ± 1 SD were reported for all parameters. Linear and multiple linear regressions were performed to correlate the GTV-based parameters (SUV_{max}, SUV_{mean}, TBR, HF, and HV) and to quantify the voxel-wise comparison of the FDG and HX4 uptake. Pearson correlation coefficients were calculated. A P value of <0.05 was assumed to be statistically significant.

Results

Overall correlation of FDG and HX4 parameters

This study analyzed the overall FDG and HX4 uptake in the primary tumor and lymph nodes of 25 patients with NSCLC. All GTV_{prim} ($N = 25$) and 19 GTV_{ln} were larger than 5 cm^3 and all were used for the analysis. The average values of the GTV, FDG, and HX4 parameters are shown in Table 1. The subclassification, based on tumor pathology, showed no significant differences for any of the FDG

Table 1. FDG- and HX4-uptake parameters (mean ± SD) for the primary lesions (GTV_{prim}) and involved lymph nodes (GTV_{ln})

			FDG				HX4				
	N	Volume GTV	SUV_{mean}	SUV_{max}	HF	HV	SUV_{mean}	SUV_{max}	TBR_{max}	HF	HV
GTV_{prim} average	25	127 ± 173 cm^3	5.3 ± 2.5	13.3 ± 6.6	41 ± 21%	36 ± 33 cm^3	0.8 ± 0.3	1.3 ± 0.4	1.8 ± 0.6	14 ± 15%	18 ± 30 cm^3
(range)		(6–852 cm^3)	(1.7–10.9)	(3.5–30.4)	(10%–85%)	(5–123 cm^3)	(0.4–1.2)	(0.6–2.1)	(0.9–3.5)	(0%–49%)	(0–131 cm^3)
GTV_{ln} average	19	57 ± 72 cm^3	3.9 ± 1.5	9.3 ± 4.0	49 ± 22%	29 ± 40 cm^3	0.7 ± 0.2	1.1 ± 0.4	1.7 ± 0.5	7 ± 10%	7 ± 13 cm^3
(range)		(7–254 cm^3)	(1.3–6.7)	(2.4–18.5)	(20%–92%)	(2–139 cm^3)	(0.4–1.0)	(0.5–1.8)	(1.1–2.8)	(0%–37%)	(0–46 cm^3)

Published OnlineFirst October 14, 2014; DOI: 10.1158/1078-0432.CCR-14-1524

Table 2. Pearson correlation coefficient (*R*) and corresponding *P* values of GTV_{prim}-based parameters on FDG- and HX4-PET

	Volume GTV_{prim}	HX4-SUV_{mean}	HX4-SUV_{max}	HX4-TBR_{max}	HX4-HF	HX4-HV
Volume GTV_{prim}						
R	—	0.16	0.48	0.49	0.01	0.60
P	—	0.48	0.02	0.01	0.95	<0.01
FDG-SUV_{mean}						
R	0.13	0.52	0.58	0.46	0.44	0.52
P	0.54	0.01	<0.01	0.02	0.03	<0.01
FDG-SUV_{max}						
R	0.47	0.39	0.54	0.55	0.28	0.66
P	0.02	0.07	<0.01	<0.01	0.17	<0.001
FDG-HF						
R	−0.47	0.20	0.02	−0.14	0.31	−0.18
P	0.02	0.36	0.93	0.49	0.13	0.40
FDG-HV						
R	0.83	0.32	0.61	0.64	0.28	0.76
P	<0.0001	0.14	<0.01	<0.01	0.18	<0.0001

or HX4 parameters (examples are shown in Supplementary Fig. S1). The FDG-HV was larger than the HX4-HV in 24/25 GTV_{prim} and in all GTV_{ln}. Potential correlations between FDG- and HX4-PET-based parameters were investigated.

The correlation coefficients for the primary tumors are shown in Table 2. The majority of the FDG- and HX4-PET-based parameters showed a significant correlation with the primary tumor volume. Note that the HX4-HV was significantly correlated with the tumor volume, while the HX4-HF was not. The FDG-SUV_{mean} correlated positively with all HX4-PET parameters. The FDG-SUV_{max} only showed a significant correlation with HX4-SUV_{max} ($R = 0.54$; $P < 0.01$), HX4-TBR ($R = 0.55$; $P < 0.01$), and HX4-HV ($R = 0.66$; $P < 0.001$). The highest correlations were observed when comparing the FDG-HV with the HX4-based parameters: HX4-SUV_{max} ($R = 0.63$; $P < 0.01$), HX4-TBR ($R = 0.62$; $P < 0.01$), and HX4-HV ($R = 0.76$; $P < 0.0001$). Two examples are shown in Fig. 1. From Fig. 1B one can appreciate that, although there is a correlation between FDG-SUV_{max} and HX4-TBR_{max}, it is not possible to distinguish the nonhypoxic lesions by using only the FDG-SUV_{max} parameter.

A multiple linear regression was performed to test the interaction between primary tumor volume and FDG parameters to predict the hypoxic volume. Using the parameters primary tumor volume and FDG-SUV_{max} to predict HX4-HV, we observed a correlation coefficient of 0.74 ($R^2 = 0.55$) with a significant contribution of both FDG-SUV_{max} ($P < 0.01$) and primary tumor volume ($P = 0.03$). Adding the interaction term (FDG-SUV_{max}* primary tumor volume) to the model increases the correlation coefficient to 0.82 ($R^2 = 0.67$).

For the *involved lymph nodes*, GTV_{ln} volume has a large effect on the correlation coefficients between the HX4 and FDG parameters (Supplementary Table S2). The multiple linear regression using GTV_{ln} volume and FDG-SUV_{max} to predict HX4-HV ($R = 0.96$) therefore showed a significant contribution only for the GTV_{ln} volume ($P < 0.001$) and not for FDG-SUV_{max} ($P = 0.26$).

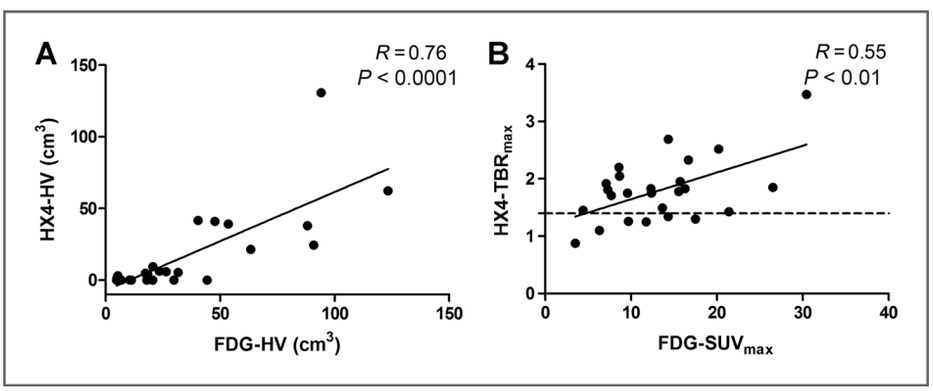

Figure 1. Comparison between FDG- and HX4-PET based parameters: A, FDG-HV versus HX4-HV and B, FDG-SUV_{max} versus HX4-TBR. The dashed line shows the threshold to define hypoxia (HX4-$TBR_{max} = 1.4$).

Published OnlineFirst October 14, 2014; DOI: 10.1158/1078-0432.CCR-14-1524

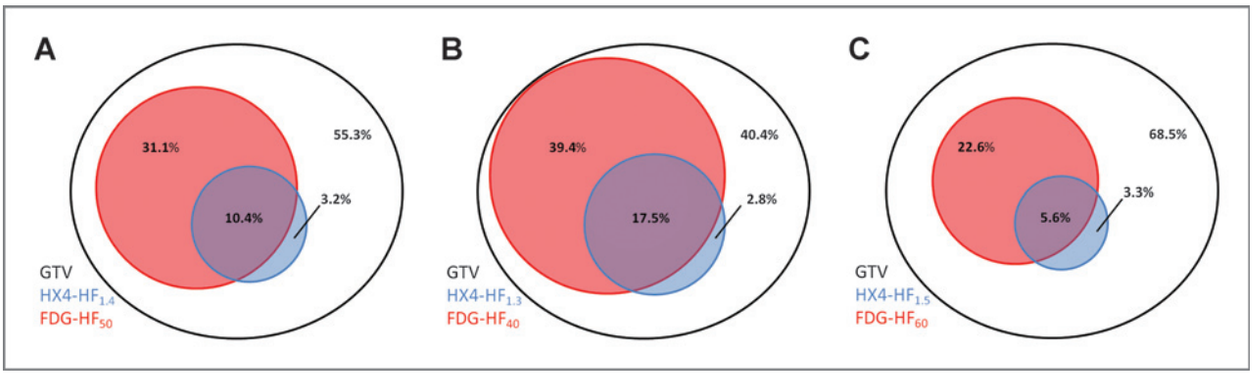

Figure 2. Visualization of the overlap between FDG-HF and HX4-HF. A, using the standard thresholds TBR > 1.4 (HX4) and SUV > 50%SUV_{max} (FDG). B, using alternative thresholds TBR > 1.3 (HX4) and SUV > 40% of SUV_{max} (FDG). C, using the alternative thresholds TBR > 1.5 (HX4) and SUV > 60% of SUV_{max} (FDG).

Average distribution of FDG and HX4 uptake

The average distribution within the primary tumor based on the four previously predefined categories is shown in Table 3 and visualized in Fig. 2A. On average, the FDG-HV is 42% ± 21% of the GTV_{prim}, of which 10% ± 12% is hypoxic. On average, 3% (range, 0%–31%) of the GTV_{prim} is hypoxic but outside the FDG-HV, representing 24% (3.2%/13.6%) of the total hypoxic volume.

The effect of alternative thresholds on the average distribution of FDG and HX4 within the primary tumor is shown in Supplementary Table S3 and visualized for two examples in Fig. 2B and C. This figure shows that the hypoxic percentage of the GTV (HX4-HF) outside the high FDG area (FDG-HF) is relatively stable.

Spatial correlation of FDG- and HX4-uptake patterns

Tracer uptake above the background level in both PET scans is essential for comparing the overlap of FDG-HV and HX4-HV. All primary lesions showed FDG uptake with an SUV_{max} > 3.5; however, only 19 out of 25 primary lesions expressed an HX4 uptake (TBR > 1.4). These 19 lesions were selected for further analysis.

On the basis of the voxel-wise analysis, we observed that in 10 lesions, less than 1 cm^3 of the HX4-HV was outside the FDG-HV (group 1; Fig. 3A). In seven lesions, 2 to 12 cm^3 of the HX4-HV was outside the FDG-HV (group 2; Fig. 3B). Finally, in 2 patients, a clearly distinct uptake pattern was observed between the two tracers and hypoxic volumes of 46 and 102 cm^3 were observed outside the FDG high-uptake region, which were 73% and 78% of the total HX4-HF, respectively (group 3; Fig. 3C). The primary tumor volume was significantly correlated to the group the lesion was assigned to ($R = 0.75$; $P < 0.01$).

Discussion

This study was initiated to assess the correlation of (spatial) uptake patterns of hypoxia (using HX4-PET) and tumor metabolism (using FDG-PET) in primary NSCLC and associated lymph node metastases. Both biologic features are known to have an adverse impact on treatment outcome in NSCLC. FDG-PET is routinely used in clinical practice for staging, radiotherapy planning, and treatment response monitoring, while the use of hypoxia (HX4) PET imaging is still limited to clinical trials. We show in 25 patients with NSCLC, with different histopathologic subtypes, that HX4-PET imaging provides additional information to FDG-PET, which can be used to individualize patient treatment.

The relationship between HX4- and FDG-PET was investigated at a tumor level by comparing the overall uptake within the GTVs of the primary tumor and lymph node metastases. Significant correlations were observed between GTV-, HX4-, and FDG-PET image parameters. Previous studies comparing the overall uptake of hypoxia PET and FDG-PET showed varying results. No correlations were observed by Bollineni and colleagues (7) or Cherk and colleagues (21), while Vera and colleagues (22) reported a significant correlation. Gagel and colleagues (23) compared FDG and FMISO uptake to the gold standard of hypoxia measurements (pO_2 polarography) and observed a moderate correlation for FMISO but no correlation for FDG. However, because both FDG-SUV_{max} and GTV are

Table 3. Average distribution of high and low HX4 and FDG uptake within the GTV_{prim}

Overlap between	FDG-low	FDG-high	GTV
HX4-low	(i) 55.3 ± 21.9% (8.5%–89.8%)	(ii) 31.1 ± 19.5% (9.8%–84.3%)	86.4 ± 15.5 (50.7%–100%)
HX4-high	(iii) 3.2 ± 6.5% (0%–31.0%)	(iv) 10.4 ± 12.2% (0%–43.4%)	13.6 ± 15.5 (0%–49.3%)
GTV	58.5 ± 21.6% (14.6%–89.8%)	41.5 ± 21.2% (10.2%–85.4%)	100%

NOTE: Standard thresholds were used: TBR > 1.4 (HX4) and SUV > 50%SUV_{max} (FDG).

Published OnlineFirst October 14, 2014; DOI: 10.1158/1078-0432.CCR-14-1524

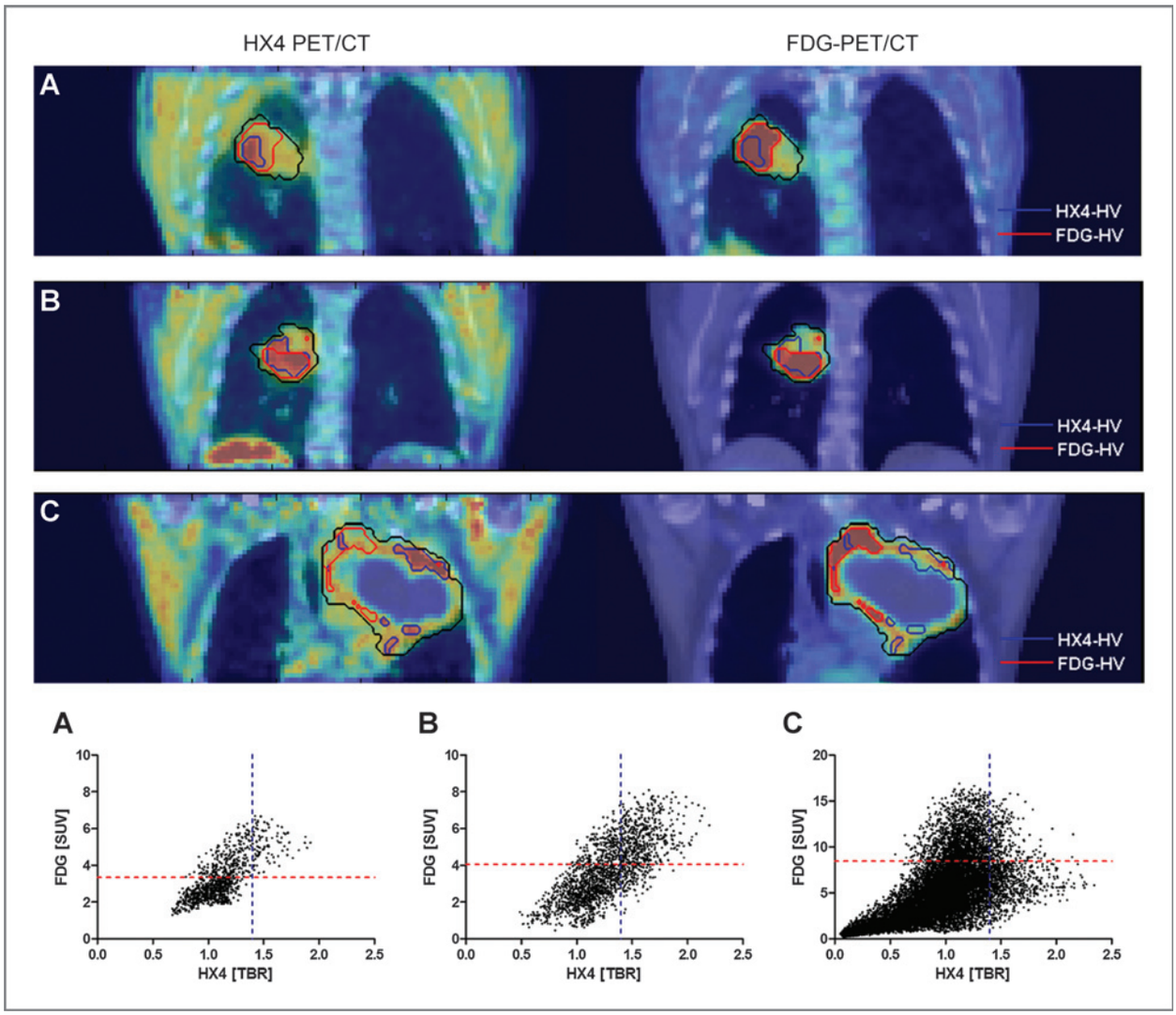

Figure 3. Visual and voxel-wise comparison of HX4 and FDG-PET/CT. A, HX4-HV within the FDG-HV. B, partial overlap between HX4-HV and FDG-HV. C, two distinct uptake patterns.

predictors of survival in NSCLC (24–26) and the amount of tumor hypoxia is related to outcome after radiotherapy (27), the reported correlation between hypoxia and FDG-PET is plausible.

Information about hypoxia on a tumor level can be used in clinical practice to select patients who may benefit from hypoxia modification before or during anticancer treatment. Previous studies have shown that the addition of hypoxic modification during radiotherapy results in an increased therapeutic benefit (28). Recently, Arrieta and colleagues (29) investigated in patients with NSCLC the use of nitroglycerin (an organic nitrate that causes vasodilatation, increased blow flow, and reduces the expression of HIF1-α) in combination with chemoradiation. In this study, promising response rates were observed; however, there was also (mild) increased toxicity (e.g., headache, hypotension) due to nitroglycerin administration. Another promising compound is the hypoxia-activated prodrug TH-302 that releases bromo isophosphoramide mustard, a potent DNA-alkylating agent, in hypoxic regions. Saggar and Tannock (30) recently demonstrated that TH-302 administered together with chemotherapy enhances the antitumor effect but also increases toxicity. From these recent studies, we acknowledge the therapeutic effect of additional antihypoxia treatment, but also the importance to limit unnecessary toxicity by selecting patients who will benefit from these modifications. We show that we can noninvasively visualize and quantify tumor hypoxia, using HX4-PET, in patients with NSLSC. In addition, our results show that patients with a larger tumor size and higher FDG uptake are more likely to have a larger hypoxic volume. This combination (GTV size and FDG uptake) could be used as a surrogate for hypoxia PET imaging; however, despite the correlation between hypoxia and FDG parameters, the

Published OnlineFirst October 14, 2014; DOI: 10.1158/1078-0432.CCR-14-1524

distinction between hypoxic and nonhypoxic tumors based on FDG-PET can be misleading, because nonhypoxic tumors are present in a broad range of FDG uptake (FDG-SUV_{max}, 3.5–17.5 also shown in Fig. 1B).

It is important to note that a correlation at a global tumor level provides no information about the intratumoral heterogeneity. At the moment, limited data are available concerning the correlation of hypoxia PET and FDG-PET at a subvolume (e.g., voxel) level in NSCLC (7, 31). The spatial concordance and discordance of both PET modalities is of interest for radiotherapy boosting strategies. FDG-PET is already used in the context of clinical trials to boost highly metabolic tumor subvolumes (18, 32). We hypothesize that hypoxia PET imaging may be more selective in defining radioresistant voxels within the GTV, and can provide complementary information regarding the definition of radiotherapy boost volumes. A voxel-wise comparison was performed to evaluate the spatial distribution of the HX4 and FDG uptake. A reasonable correlation between both tracers was observed in the majority of patients. This is in contradiction to the previous published results of Bollineni and colleagues (7), who observed no correlation between FDG and the hypoxia PET tracer FAZA. This disagreement can probably be explained by the definition of the target lesion. Bollineni and colleagues used an FDG-based threshold to define the target lesion, thereby excluding voxels with a low FDG uptake. Conversely, Lohith and colleagues (31) reported a similar spatial distribution of [^{62}Cu]ATSM and FDG in 5 patients with an adenocarcinoma of the lung, which was not present in patients with SCC. Also, they observed a difference in intratumoral distribution between adenocarcinoma and SCC, which was not observed in our cohort of patients with NSCLC. It is well described that hypoxia leads to an increased uptake of glucose through various molecular mechanisms (33). Nevertheless, an increased glycolysis is also observed without hypoxia, e.g., by c-myc aberrations (34). From a molecular point of view, it is therefore logical that FDG uptake and hypoxia is partially overlapping and is highly dependent on the genetics of the tumor.

Thresholds were defined arbitrarily to define regions with a high or low uptake on both FDG- and HX4-PET. The high FDG-PET volume was defined on the basis of the ongoing NSCLC boost trial (18), whereas the high HX4 region was based on previous publications, indicating that a threshold of TBR>1.4 is rational to define hypoxia (6, 8, 35, 36). These thresholds showed the HX4-HV to be three times smaller on average than the FDG-HV.

This work can be used in clinical setting to divide patients with a hypoxic lesion into different groups, stratifying lesions with an agreement or disagreement between the HX4- and FDG-PET-uptake pattern. In the patients with a concordance, the use of HX4-PET has limited additional value for the selection of the radiotherapy boost volume; however, this volume could be limited to HX4-high areas only, facilitating further dose escalation without comprising the surrounding healthy tissue. In other patients, a (partial) discordance between the HX4- and FDG-PET-uptake pattern was observed. In these patients, the boost region could be adjusted to either HX4-PET or a combination of HX4- and FDG-PET with the aim to improve locoregional control. On the basis of the current analysis, a radiation boost to the FDG-high area (SUV > 50% SUV_{max}) would on average miss 24% of the hypoxic volume, which seems in agreement with the residual activity after radiotherapy outside the high-FDG area as reported by Aerts and colleagues (11). Previous studies have already shown that radiotherapy dose distribution based on tumor hypoxia is possible and promising (37, 38). Currently, there are strategies available to investigate the original location of local recurrences inside the tumor volume (39). These studies will characterize the subvolumes inside the heteregenous tumor that are difficult to control. Ultimately, the effect of tumor subvolume characterization and targeting, by radiotherapy or other therapeutic interventions, needs to be assessed in a randomized trial.

This study has several limitations. First, most patients received chemotherapy before the start of radiotherapy and PET imaging. Chemotherapy can reduce the amount of tumor hypoxia and downregulates metabolism, resulting in a decreased uptake of HX4 and FDG (40). However, the focus of our research is on the correlation between both imaging modalities; therefore, treatment differences between patients are less relevant. In addition, it is most important to have recent PET information before the start of (adaptive) radiotherapy. Second, we were not able to validate the current imaging observations on tumor specimens. Nevertheless, van Baardwijk and colleagues (41) showed previously that FDG-PET imaging is correlated to GLUT-1 and HIF-1α expression in patients with NSCLC and Dubois and colleagues (8) showed a high correlation between HX4-PET uptake and pimonidazole staining in a rat rhabdomyosarcoma model. Third, the study acquired PET scans in free-breathing, which might cause blurring of the PET signal. Although, both the FDG and HX4 scans were obtained in this setting, we do not expect any substantial bias for the comparison. Furthermore, advanced-stage tumors are known to show little breathing-induced motion (42, 43). Fourth, the FDG-PET/CT was rigidly registered to the HX4-PET/CT scan to compare spatial uptake patterns. Small errors in registration can have a significant effect on correlation (44). However, patients in the current study were aligned in radiotherapy treatment position providing a strong basis for accurate registration. Fifth, there was a small time interval between the FDG- and HX4-PET/CT scan. Changes in anatomy, tumor metabolism, or hypoxia may have occurred in this interval and influenced the comparison results. The time interval in our study was short (median, 3 days) and no interventions (e.g., chemotherapy or radiotherapy) were performed between the two scans, limiting the chances of anatomic or physiologic changes. Finally, the usability of a tracer for radiation dose painting is dependent on its spatial reproducibility. Aerts and colleagues (45) showed that the location of low and high FDG volumes was stable during radiotherapy. The short-time reproducibility for HX4 (2 vs. 4 hours) was confirmed, but

Published OnlineFirst October 14, 2014; DOI: 10.1158/1078-0432.CCR-14-1524

the long-term reproducibility is still unknown (6). However, a high reproducibility has been reported by Busk and colleagues (46) and Okamoto and colleagues (47) for the alternative hypoxia tracers FMISO and FAZA.

In conclusion, there is a positive correlation between GTV-, FDG-, and HX4-uptake parameters on a tumor level. The hypoxic tumor volume is on average three times smaller than the metabolic active tumor volume. Approximately half of the lesions showed a good spatial correlation between the PET tracers. In the other cases, a (partial) mismatch was observed. Hypoxia PET imaging gives complimentary information to metabolic FDG imaging, which can potentially be used to individualize patient treatment by selecting patients for treatment with hypoxic sensitizers or hypoxia PET-based radiotherapy dose escalation.

Disclosure of Potential Conflicts of Interest

No potential conflicts of interest were disclosed.

Authors' Contributions

Conception and design: C.M.L. Zegers, W. van Elmpt, B. Reymen, M.C. Öllers, F.M. Mottaghy, D. De Ruysscher, P. Lambin

Development of methodology: C.M.L. Zegers, W. van Elmpt, E.G.C. Troost, A.D. Windhorst, P. Lambin

Acquisition of data (provided animals, acquired and managed patients, provided facilities, etc.): C.M.L. Zegers, W. van Elmpt, B. Reymen, A.J.G. Even, F.J.P. Hoebers, J. Eriksson, A.D. Windhorst, F.M. Mottaghy, D. De Ruysscher

Analysis and interpretation of data (e.g., statistical analysis, biostatistics, computational analysis): C.M.L. Zegers, W. van Elmpt, A.J.G. Even, E.G.C. Troost, M.C. Öllers, R.M.A. Houben, F.M. Mottaghy, P. Lambin

Writing, review, and/or revision of the manuscript: C.M.L. Zegers, W. van Elmpt, B. Reymen, A.J.G. Even, E.G.C. Troost, M.C. Öllers, F.J.P. Hoebers, R.M.A. Houben, J. Eriksson, A.D. Windhorst, F.M. Mottaghy, D. De Ruysscher, P. Lambin

Administrative, technical, or material support (i.e., reporting or organizing data, constructing databases): C.M.L. Zegers, W. van Elmpt, J. Eriksson

Study supervision: W. van Elmpt, P. Lambin

Acknowledgments

The authors thank the patients who agreed to participate, C. Overhof for handling the data management for both clinical trials, and R. Franssen for the data acquisition.

Grant Support

This study was financially supported by the CTMM framework (AIRFORCE project, grant 030-103), the EU 6th and 7th framework program (METOXIA, EURECA, and ARTFORCE), euroCAT (IVA Interreg; www.eurocat.info), and the Kankeronderzoekfonds Limburg of the Health Foundation Limburg and the Dutch Cancer Society (KWF UM 2011-5020, KWF UM 2009-4454, KWF MAC 2011-4970, and KWF MAC 2013-6425).

The costs of publication of this article were defrayed in part by the payment of page charges. This article must therefore be hereby marked *advertisement* in accordance with 18 U.S.C. Section 1734 solely to indicate this fact.

Received June 13, 2014; revised September 18, 2014; accepted October 6, 2014; published OnlineFirst October 14, 2014.

References

1. Siegel R, Naishadham D, Jemal A. Cancer statistics, 2013. CA Cancer J Clin 2013;63:11–30.
2. Auperin A, Le Pechoux C, Rolland E, Curran WJ, Furuse K, Fournel P, et al. Meta-analysis of concomitant versus sequential radiochemotherapy in locally advanced non–small-cell lung cancer. J Clin Oncol 2010;28:2181–90.
3. Nordsmark M, Bentzen SM, Rudat V, Brizel D, Lartigau E, Stadler P, et al. Prognostic value of tumor oxygenation in 397 head and neck tumors after primary radiation therapy. An international multi-center study. Radiother Oncol 2005;77:18–24.
4. Zips D, Zophel K, Abolmaali N, Perrin R, Abramyuk A, Haase R, et al. Exploratory prospective trial of hypoxia-specific PET imaging during radiochemotherapy in patients with locally advanced head-and-neck cancer. Radiother Oncol 2012;105:21–8.
5. Milosevic M, Warde P, Menard C, Chung P, Toi A, Ishkanian A, et al. Tumor hypoxia predicts biochemical failure following radiotherapy for clinically localized prostate cancer. Clin Cancer Res 2012;18:2108–14.
6. Zegers CM, van Elmpt W, Wierts R, Reymen B, Sharifi H, Ollers MC, et al. Hypoxia imaging with [(18)F]HX4 PET in NSCLC patients: defining optimal imaging parameters. Radiother Oncol 2013;109:58–64.
7. Bollineni VR, Kerner GS, Pruim J, Steenbakkers RJ, Wiegman EM, Koole MJ, et al. PET imaging of tumor hypoxia using 18F-fluoroazomycin arabinoside in stage III–IV non–small cell lung cancer patients. J Nucl Med 2013;54:1175–80.
8. Dubois LJ, Lieuwes NG, Janssen MH, Peeters WJ, Windhorst AD, Walsh JC, et al. Preclinical evaluation and validation of [18F]HX4, a promising hypoxia marker for PET imaging. Proc Natl Acad Sci U S A 2011;108:14620–5.
9. van Loon J, Janssen MH, Ollers M, Aerts HJ, Dubois L, Hochstenbag M, et al. PET imaging of hypoxia using [18F]HX4: a phase I trial. Eur J Nucl Med Mol Imaging 2010;37:1663–8.
10. Chen L, Zhang Z, Kolb HC, Walsh JC, Zhang J, Guan Y. (1)(8)F-HX4 hypoxia imaging with PET/CT in head and neck cancer: a comparison with (1)(8)F-FMISO. Nucl Med Commun 2012;33:1096–102.
11. Aerts HJ, van Baardwijk AA, Petit SF, Offermann C, Loon J, Houben R, et al. Identification of residual metabolic-active areas within individual NSCLC tumours using a pre-radiotherapy (18)Fluorodeoxyglucose-PET-CT scan. Radiother Oncol 2009;91:386–92.
12. Abramyuk A, Tokalov S, Zophel K, Koch A, Szluha Lazanyi K, Gillham C, et al. Is pre-therapeutical FDG-PET/CT capable to detect high risk tumor subvolumes responsible for local failure in non–small cell lung cancer? Radiother Oncol 2009;91:399–404.
13. Spijkerman J, Fontanarosa D, Das M, van Elmpt W. Validation of nonrigid registration in pretreatment and follow-up PET/CT scans for quantification of tumor residue in lung cancer patients. J Appl Clin Med Phys 2014;15:4847.
14. Lambin P, van Stiphout RG, Starmans MH, Rios-Velazquez E, Nalbantov G, Aerts HJ, et al. Predicting outcomes in radiation oncology—multifactorial decision support systems. Nat Rev Clin Oncol 2013;10:27–40.
15. Aerts HJ, Lambin P, Ruysscher DD. FDG for dose painting: a rational choice. Radiother Oncol 2010;97:163–4.
16. Lambin P, Petit SF, Aerts HJ, van Elmpt WJ, Oberije CJ, Starmans MH, et al. The ESTRO Breur Lecture 2009. From population to voxel-based radiotherapy: exploiting intra-tumour and intra-organ heterogeneity for advanced treatment of non–small cell lung cancer. Radiother Oncol 2010;96:145–52.
17. Pereira KM, Chaves FN, Viana TS, Carvalho FS, Costa FW, Alves AP, et al. Oxygen metabolism in oral cancer: HIF and GLUTs (review). Oncol Lett 2013;6:311–6.
18. van Elmpt W, De Ruysscher D, van der Salm A, Lakeman A, van der Stoep J, Emans D, et al. The PET-boost randomised phase II dose-escalation trial in non–small cell lung cancer. Radiother Oncol 2012;104:67–71.

Published OnlineFirst October 14, 2014; DOI: 10.1158/1078-0432.CCR-14-1524

19. Doss M, Zhang JJ, Belanger MJ, Stubbs JB, Hostetler ED, Alpaugh K, et al. Biodistribution and radiation dosimetry of the hypoxia marker 18F-HX4 in monkeys and humans determined by using whole-body PET/CT. Nucl Med Commun 2010;31:1016–24.
20. Boellaard R, Oyen WJ, Hoekstra CJ, Hoekstra OS, Visser EP, Willemsen AT, et al. The Netherlands protocol for standardisation and quantification of FDG whole body PET studies in multi-centre trials. Eur J Nucl Med Mol Imaging 2008;35:2320–33.
21. Cherk MH, Foo SS, Poon AM, Knight SR, Murone C, Papenfuss AT, et al. Lack of correlation of hypoxic cell fraction and angiogenesis with glucose metabolic rate in non–small cell lung cancer assessed by 18F-fluoromisonidazole and 18F-FDG PET. J Nucl Med 2006;47:1921–6.
22. Vera P, Bohn P, Edet-Sanson A, Salles A, Hapdey S, Gardin I, et al. Simultaneous positron emission tomography (PET) assessment of metabolism with (1)(8)F-fluoro-2-deoxy-d-glucose (FDG), proliferation with (1)(8)F-fluoro-thymidine (FLT), and hypoxia with (1)(8)fluoro-misonidazole (F-miso) before and during radiotherapy in patients with non–small-cell lung cancer (NSCLC): a pilot study. Radiother Oncol 2011;98:109–16.
23. Gagel B, Piroth M, Pinkawa M, Reinartz P, Zimny M, Kaiser HJ, et al. pO polarography, contrast enhanced color duplex sonography (CDS), [18F] fluoromisonidazole and [18F] fluorodeoxyglucose positron emission tomography: validated methods for the evaluation of therapy-relevant tumor oxygenation or only bricks in the puzzle of tumor hypoxia? BMC Cancer 2007;7:113.
24. Cistaro A, Quartuccio N, Mojtahedi A, Fania P, Filosso PL, Campenni A, et al. Prediction of 2 years-survival in patients with stage I and II non–small cell lung cancer utilizing (18)F-FDG PET/CT SUV quantification. Radiol Oncol 2013;47:219–23.
25. Tanaka H, Hayashi S, Hoshi H. Pretreatment maximum standardized uptake value on 18F-fluorodeoxyglucose positron emission tomography is a predictor of outcome for stage I non–small cell lung cancer after stereotactic body radiotherapy. Asia Pac J Clin Oncol 2013.
26. Satoh Y, Onishi H, Nambu A, Araki T. Volume-based parameters measured by using FDG PET/CT in patients with stage I NSCLC treated with stereotactic body radiation therapy: prognostic value. Radiology 2014;270:275–81.
27. Eschmann SM, Paulsen F, Reimold M, Dittmann H, Welz S, Reischl G, et al. Prognostic impact of hypoxia imaging with 18F-misonidazole PET in non–small cell lung cancer and head and neck cancer before radiotherapy. J Nucl Med 2005;46:253–60.
28. Overgaard J. Hypoxic modification of radiotherapy in squamous cell carcinoma of the head and neck–a systematic review and meta-analysis. Radiother Oncol 2011;100:22–32.
29. Arrieta O, Blake M, de la Mata-Moya MD, Corona F, Turcott J, Orta D, et al. Phase II study. Concurrent chemotherapy and radiotherapy with nitroglycerin in locally advanced non–small cell lung cancer. Radiother Oncol 2014;111:311–5.
30. Saggar JK, Tannock IF. Activity of the hypoxia-activated pro-drug TH-302 in hypoxic and perivascular regions of solid tumors and its potential to enhance therapeutic effects of chemotherapy. Int J Cancer 2014;134:2726–34.
31. Lohith TG, Kudo T, Demura Y, Umeda Y, Kiyono Y, Fujibayashi Y, et al. Pathophysiologic correlation between 62Cu-ATSM and ^{18}F-FDG in lung cancer. J Nucl Med 2009;50:1948–53.
32. Moller DS, Khalil AA, Knap MM, Muren LP, Hoffmann L. A planning study of radiotherapy dose escalation of PET-active tumour volumes in non–small cell lung cancer patients. Acta Oncol 2011;50:883–8.
33. Vander Heiden MG, Cantley LC, Thompson CB. Understanding the Warburg effect: the metabolic requirements of cell proliferation. Science 2009;324:1029–33.
34. Dang CV, Le A, Gao P. MYC-induced cancer cell energy metabolism and therapeutic opportunities. Clin Cancer Res 2009;15:6479–83.
35. Dubois L, Landuyt W, Haustermans K, Dupont P, Bormans G, Vermaelen P, et al. Evaluation of hypoxia in an experimental rat tumour model by [(18)F]fluoromisonidazole PET and immunohistochemistry. Br J Cancer 2004;91:1947–54.
36. Rasey JS, Koh WJ, Evans ML, Peterson LM, Lewellen TK, Graham MM, et al. Quantifying regional hypoxia in human tumors with positron emission tomography of [18F]fluoromisonidazole: a pretherapy study of 37 patients. Int J Radiat Oncol Biol Phys 1996;36:417–28.
37. Petit SF, Dekker AL, Seigneuric R, Murrer L, van Riel NA, Nordsmark M, et al. Intra-voxel heterogeneity influences the dose prescription for dose-painting with radiotherapy: a modelling study. Phys Med Biol 2009;54:2179–96.
38. Thorwarth D, Eschmann SM, Paulsen F, Alber M. Hypoxia dose painting by numbers: a planning study. Int J Radiat Oncol Biol Phys 2007;68:291–300.
39. Due AK, Vogelius IR, Aznar MC, Bentzen SM, Berthelsen AK, Korreman SS, et al. Recurrences after intensity modulated radiotherapy for head and neck squamous cell carcinoma more likely to originate from regions with high baseline [18F]-FDG uptake. Radiother Oncol 2014;111:360–5.
40. Bittner MI, Wiedenmann N, Bucher S, Hentschel M, Mix M, Weber WA, et al. Exploratory geographical analysis of hypoxic subvolumes using ^{18}F-MISO-PET imaging in patients with head and neck cancer in the course of primary chemoradiotherapy. Radiother Oncol 2013;108:511–6.
41. van Baardwijk A, Dooms C, van Suylen RJ, Verbeken E, Hochstenbag M, Dehing-Oberije C, et al. The maximum uptake of (18)F-deoxyglucose on positron emission tomography scan correlates with survival, hypoxia inducible factor-1alpha and GLUT-1 in non–small cell lung cancer. Eur J Cancer 2007;43:1392–8.
42. Bosmans G, van Baardwijk A, Dekker A, Ollers M, Boersma L, Minken A, et al. Intra-patient variability of tumor volume and tumor motion during conventionally fractionated radiotherapy for locally advanced non–small-cell lung cancer: a prospective clinical study. Int J Radiat Oncol Biol Phys 2006;66:748–53.
43. Yu ZH, Lin SH, Balter P, Zhang L, Dong L. A comparison of tumor motion characteristics between early stage and locally advanced stage lung cancers. Radiother Oncol 2012;104:33–8.
44. Nyflot MJ, Harari PM, Yip S, Perlman SB, Jeraj R. Correlation of PET images of metabolism, proliferation and hypoxia to characterize tumor phenotype in patients with cancer of the oropharynx. Radiother Oncol 2012;105:36–40.
45. Aerts HJ, Bosmans G, van Baardwijk AA, Dekker AL, Oellers MC, Lambin P, et al. Stability of 18F-deoxyglucose uptake locations within tumor during radiotherapy for NSCLC: a prospective study. Int J Radiat Oncol Biol Phys 2008;71:1402–7.
46. Busk M, Mortensen LS, Nordsmark M, Overgaard J, Jakobsen S, Hansen KV, et al. PET hypoxia imaging with FAZA: reproducibility at baseline and during fractionated radiotherapy in tumour-bearing mice. Eur J Nucl Med Mol imaging 2013;40:186–97.
47. Okamoto S, Shiga T, Yasuda K, Ito YM, Magota K, Kasai K, et al. High reproducibility of tumor hypoxia evaluated by 18F-fluoromisonidazole PET for head and neck cancer. J Nucl Med 2013;54:201–7.

Published OnlineFirst October 14, 2014; DOI: 10.1158/1078-0432.CCR-14-1524

Clinical Cancer Research

In Vivo Quantification of Hypoxic and Metabolic Status of NSCLC Tumors Using [^{18}F]HX4 and [^{18}F]FDG-PET/CT Imaging

Catharina M.L. Zegers, Wouter van Elmpt, Bart Reymen, et al.

Clin Cancer Res 2014;20:6389-6397. Published OnlineFirst October 14, 2014.